Trigonal Prismatic Structure of Tris(butadiene)molybdenum and Related Complexes Revisited: Diolefin or Metallacyclopentene Coordination?

Martin Kaupp,*,† Thomas Kopf,† Alexander Murso,† Dietmar Stalke,† Carsten Strohmann,† John R. Hanks,‡ F. Geoffrey N. Cloke,‡ and Peter B. Hitchcock‡

Institut für Anorganische Chemie, Universität Würzburg, Am Hubland, D-97074 Würzburg, Germany, and School of Chemistry, Physics, and Environmental Science, University of Sussex, Falmer, Brighton BN1 9Q, United Kingdom

Received July 3, 2002

The unusual trigonal prismatic structure of tris(butadiene)molybdenum, reported in 1975 by Skell, has been revisited by extensive quantum chemical calculations and by a low-temperature single-crystal X-ray diffraction study. While a trigonal prismatic coordination arrangement is confirmed by DFT and MP2 structure optimizations, the calculations provide very different bond lengths than earlier crystallographic studies: Due to appreciable back-bonding, the terminal Mo−C1 bonds are significantly shorter than the central Mo−C2 bonds (ca. 2.29 vs ca. 2.36 Å), and the central (C2−C2A) bonds are actually shorter than the terminal ones (ca. 1.40 vs ca. 1.44 Å), as found previously for substituted complexes. Similar structures have been computed for tris(butadiene)tungsten and for related, substituted systems. A structure redetermination of tris(butadiene)molybdenum at low temperature shows that the erroneous bond lengths obtained previously are due to the presence of a disorder resulting from the superposition of two different orientations of the three butadiene ligands with different site occupation factors. Refinement of this disorder results in a physically more plausible orientation of the anisotropic displacement parameter and gives by a factor of 10 improved estimated standard deviations for the geometrical features. A much better agreement between theory and experiment is attained. It is now obvious that resonance structures involving metallacyclopentene rings contribute significantly to bonding. This conclusion has been confirmed by natural bond orbital/natural resonance theory analyses, which indicate overall larger contributions from metallacyclopentene resonance structures than from traditional resonance structures with π-bonded diolefins. Explanations are provided for the trigonal prismatic structure preferences. MO analyses differ qualitatively and quantitatively from previous work, due to the use of refined structural parameters. Computed ligand NMR chemical shifts agree well with experimental data, provided that they are calculated at the correct structures.

Introduction

Tris(butadiene)molybdenum and -tungsten, $M(bd)_3$ (M = Mo, W), are the prototypical homoleptic transition metal butadiene complexes.[1] Apart from the general importance of butadiene complexes, e.g., in the context of catalysis, the structure of $Mo(bd)_3$ reported by Skell 27 years ago[2] has aroused interest for several reasons: (a) The arrangement of the six terminal ligand carbon atoms around the metal was found to be trigonal prismatic rather than the more common octahedral coordination; (b) the Mo−C bond lengths to terminal and central butadiene carbon atoms were essentially equal, and the C−C bonds exhibited the alternating bond lengths of free butadiene. This contrasts with the known structures of other butadiene complexes of early transition metals, where partial equalization of the terminal and central C−C bond lengths has been observed.[3,4] It also contradicts the notion, based on extended-Hückel calculations,[5] of extensive back-bonding into the low-lying π* orbitals of butadiene, which should be reflected in an equalization of bond lengths. However, a later

* Correspondence author. E-mail: kaupp@mail.uni-wuerzburg.de. Fax: +931/888-5281.
† Universität Würzburg.
‡ University of Sussex.

(1) See, for example: Elschenbroich, Ch.; Salzer, A. *Organometallic Chemistry*, 2nd ed., Verlag Chemie: Weinheim, 1992.

(2) Skell, P. S.; McGlinchey, M. J. *Angew. Chem.* **1975**, *87*, 215; *Angew. Chem., Int. Ed. Engl.* **1975**, *14*, 195.

(3) See, for example: Erker, G.; Engel, K.; Krüger, C.; Chiang, A.-P. *Chem. Ber.* **1982**, *115*, 3311. See also: Cloke, F. G.; McCamley, A. *J. Chem. Soc., Chem. Commun.* **1991**, 1470. Wang, L.-S.; Fettinger, J. C.; Poli, R.; Meunier-Prest, R. *Organometallics* **1998**, *17*, 2692. Poli, R.; Wang, L.-S. *J. Am. Chem. Soc.* **1998**, *120*, 2831, and references therein.

(4) Özkar, S.; Kreiter, C. G.; Kotzian, M. *J. Organomet. Chem.* **1995**, *494*, 115.

(5) Green, J. C.; Kelly, M. R.; Grebenik, P. D.; Briant, C. E.; McEvoy, N. A.; Mingos, D. M. P. *J. Organomet. Chem.* **1982**, *228*, 239.

10.1021/om020525v CCC: $22.00
Publication on Web 10/15/2002

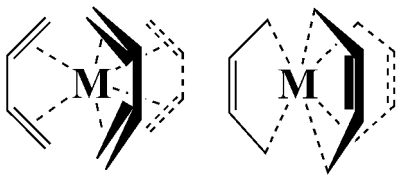

1, Mo^0, d^6 **2**, Mo^{VI}, d^0

Figure 1. Extreme resonance structures for $Mo(bd)_3$.

crystallographic reexamination by Green et al.[5] yielded the same structure as reported initially by Skell. A few years later, work by Bogdanovic et al. showed that the tris(2,3-dimethylbutadiene) complexes of molybdenum and tungsten exhibit the expected equalization of C−C bond lengths, as well as smaller terminal than central M−C bond lengths.[6] However, the structures of the unsubstituted parent complexes were not questioned.

At the time of the initial studies on $Mo(bd)_3$, trigonal prismatic coordination in transition metal complexes was largely restricted to the extended solid-state structures of some chalcogenides and pnictides[7] and to some molecular tris-dithiolene complexes.[8] During the past 10−15 years, regular or distorted trigonal prismatic coordination has been shown, both experimentally and computationally, to be much more common than previously thought.[9] The (distorted or regular) trigonal prism is the preferred structure for covalent d^0−d^2 systems when metal−ligand π-bonding is less important or absent. The distorted trigonal prismatic structure of hexamethyl tungsten, $W(CH_3)_6$, is a prototype example,[10] but many more systems are meanwhile known.[9] $Mo(bd)_3$ viewed as an Mo^0 d^6 complex with three neutral butadiene ligands (Figure 1a), as suggested by the reported structural data, has no reason to prefer a trigonal prismatic structure. In contrast, the trigonal prism becomes the natural structure for an Mo^{VI} d^0 system with three formally dianionic 2,3-butene-1,4-diyl ligands, leading to three fused metallacyclopentene rings (Figure 1b).[9] This type of electronic structure would be the expected result of extreme back-bonding. The known structures of other butadiene complexes of early transition metals[3,4,6] and the structures of some related homoleptic chelate complexes, like tris(*ortho*-xylyl)tungsten[11] or tris(methylvinyl ketone)tungsten,[12] suggest that the true structural and electronic situation should lie somewhere in the middle between these two extreme descriptions.

We therefore embarked to redetermine the solid-state structure of $Mo(bd)_3$ and of related complexes by quantum chemical calculations. As our density functional and ab initio calculations indicate the reported structural data for $Mo(bd)_3$ to be indeed inaccurate, we have carried out a low-temperature single-crystal X-ray diffraction study. The analysis of the data testifies a disorder to be present in the $Mo(bd)_3$ structure, which is otherwise isomorphous with that previously published. However, this disorder was already indicated by the orientation of the anisotropic displacement parameters (adp) previously published. The main axis of the adp's of the central carbon atoms was oriented along the central C−C bond rather than orthogonal to the main plane of the ligand. After refinement of this disorder we arrive at geometrical data that are much more in tune with the quantum chemical results and more consistent with the bonding modes discussed in this paper.

Methodological Details

Quantum Chemical Calculations. We have optimized the structures of $Mo(bd)_3$ and of $W(bd)_3$ at four different levels of theory. We used (i) Hartree−Fock (HF) calculations, (ii) second-order Møller−Plesset perturbation theory (MP2), and density functional theory, with (iii) the gradient-corrected BP86 functional,[13] and with (iv) the hybrid B3LYP functional.[14] We have furthermore optimized the structure of tris(2,3-dimethylbutadiene)molybdenum, the perfluorinated complex $Mo(C_4F_6)_3$, and all of the free ligands at the BP86 level. All structure optimizations and subsequent characterizations of stationary points on the corresponding potential energy surfaces by harmonic vibrational frequency analyses were carried out with the Gaussian98 program package.[15] Initial structure optimizations for $Mo(bd)_3$ at the BP86 DFT level were done without any symmetry restrictions, but they converged to a C_{3h} symmetrical structure (see Figure 2). Subsequent calculations employed C_{3h} symmetry for the complexes and C_{2v} symmetry for the free ligands (thus enforcing a *cis* structure in the latter case; in the case of dmbd this is a transition state, with a 41° twisted C_2 symmetrical gauge structure lower in energy by 7.6 kJ mol^{-1}). We employed quasirelativistic (QR) small-core effective-core potentials (ECPs) with (8s7p6d)/[6s5p3d] valence basis sets for the metals[16] [for comparison, calculations on $W(bd)_3$ with a corresponding nonrelativistic (NR) tung-

(6) Bogdanović, B.; Bönnemann, H.; Goddard, R.; Startsev, A.; Wallis, J. M. *J. Organomet. Chem.* **1986**, *299*, 347.

(7) See, for example: Huisman, B.; de Jonge, R.; Haas, C.; Jellinek, F. *J. Solid State Chem.* **1971**, *3*, 56, and references therein.

(8) For reviews of the early literature on tris-dithiolene complexes, see for example: (a) Eisenberg, R. *Prog. Inorg. Chem.* **1970**, *12*, 295. (b) Wentworth, R. A. D. *Coord. Chem. Rev.* **1972**, *9*, 171. For more recent reviews see, for example: (c) Martin, J. L.; Takats, J. *Can. J. Chem.* **1989**, *67*, 1914. (d) Karpishin, T. B.; Stack, T. D. P.; Raymond, K. N. *J. Am. Chem. Soc.* **1993**, *115*, 182.

(9) For a recent, comprehensive review, cf.: Kaupp, M. *Angew. Chem.* **2001**, *113*, 3642; *Angew. Chem., Int. Ed.* **2001**, *40*, 3534.

(10) (a) Pfennig, V.; Seppelt, K. *Science* **1996**, *271*, 626. (b) Kleinhenz, S.; Pfennig, V.; Seppelt, K. *Chem. Eur. J.* **1998**, *4*, 1687. (c) Kaupp, M. *J. Am. Chem. Soc.* **1996**, *118*, 3018. (d) Kaupp, M. *Chem. Eur. J.* **1999**, *4*, 1678. (e) Haaland, A.; Hammel, A.; Rypdal, K.; Volden, H. V. *J. Am. Chem. Soc.* **1990**, *112*, 4547. (f) Kang, S. K.; Tang, H.; Albright, T. A. *J. Am. Chem. Soc.* **1993**, *115*, 1971.

(11) Lappert, M. F.; Ralston, C. L.; Skelton, B. W.; White, A. H. *J. Chem. Soc., Chem. Commun.* **1981**, 485.

(12) Moriarty, R. E.; Ernst, R. D.; Bau, R. *J. Chem. Soc., Chem. Commun.* **1972**, 1242.

(13) Becke, A. D. *Phys. Rev. A* **1988**, *38*, 3098. Perdew, J. P. *Phys. Rev. B* **1986**, *33*, 8822.

(14) Becke, A. D. *J. Chem. Phys.* **1993**, *98*, 5648. Lee, C.; Yang, W.; Parr, G. R. *Phys, Rev. B* **1988**, *37*, 785. Miehlich, B.; Savin, A.; Stoll, H.; Preuss, H. *Chem. Phys. Lett.* **1989**, *157*, 200. The functional was used as implemented in the Gaussian 98 code.

(15) Frisch, M. J.; Trucks, G. W.; Schlegel, H. B.; Scuseria, G. E.; Robb, M. A.; Cheeseman, J. R.; Zakrzewski, V. G.; Montgomery, J. A., Jr.; Stratmann, R. E.; Burant, J. C.; Dapprich, S.; Millam, J. M.; Daniels, A. D.; Kudin, K. N.; Strain, M. C.; Farkas, O.; Tomasi, J.; Barone, V.; Cossi, M.; Cammi, R.; Mennucci, B.; Pomelli, C.; Adamo, C.; Clifford, S.; Ochterski, J.; Petersson, G. A.; Ayala, P. Y.; Cui, Q.; Morokuma, K.; Malick, D. K.; Rabuck, A. D.; Raghavachari, K.; Foresman, J. B.; Cioslowski, J.; Ortiz, J. V.; Baboul, A. G.; Stefanov, B. B.; Liu, G.; Liashenko, A.; Piskorz, P.; Komaromi, I.; Gomperts, R.; Martin, R. L.; Fox, D. J.; Keith, T.; Al-Laham, M. A.; Peng, C. Y.; Nanayakkara, A.; Gonzalez, C.; Challacombe, M.; Gill, P. M. W.; Johnson, B.; Chen, W.; Wong, M. W.; Andres, J. L.; Gonzalez, C.; Head-Gordon, M.; Replogle, E. S.; Pople, J. A. *Gaussian 98*, Revision A.7; Gaussian, Inc.: Pittsburgh, PA, 1998.

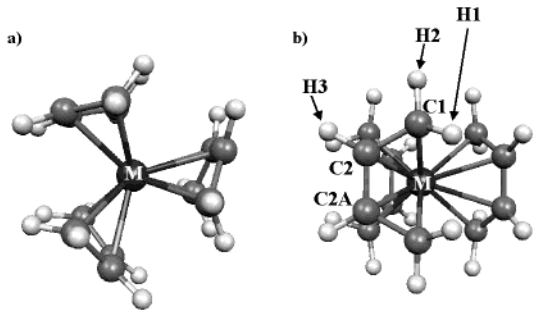

Figure 2. Quantum chemically calculated structure of $Mo(bd)_3$. (a) Top view, along C_3 axis. (b) Side view with atom labels.

sten ECP were also carried out]. ECPs and (4s4p1d)/[2s2p1d] valence basis sets were used for C and F[17,18] and a (5s1p)/[2s1p] basis for hydrogen (with a polarization p-exponent $\alpha = 0.75$).[19] Natural bond orbital (NBO) analyses[20] used the built-in NBO-3.0 routines of the Gaussian98 package. Natural resonance theory (NRT) analyses[21] made use of a more recent version of the NBO program (NBO-4.M[22]).

^{13}C and ^{1}H NMR nuclear shieldings were calculated at the sum-over-states density functional perturbation theory (SOS-DFPT) level[23−25] in its Loc1 approximation, at the BP86 optimized structures (unless noted otherwise), using the deMon-KS[25] and deMon-NMR[25] codes. We used the PW91 gradient-corrected functional[26] and employed individual gauges for localized orbitals (IGLO[27]). The quasirelativistic ECPs and valence basis sets for the metals were the same as those used in the structure optimizations (cf. above). IGLO-II all-electron basis sets[27] were used for the ligand atoms. Density and exchange−correlation potential fitting auxiliary basis sets were of the sizes 3,4 (Cr, Mo, W), 5,2 (C), and 5,1 (H) (*n*,*m* denotes *n* s-functions and *m* spd-shells with shared exponents[24]). All six Cartesian components of d-basis functions were kept. The IGLO procedure employed the Boys localization scheme.[28] For comparison to experiment, the calculated ^{13}C and ^{1}H absolute shieldings were converted to relative shifts, δ, using the absolute shieldings calculated at the same computational level for $Si(CH_3)_4$, TMS (187.4 ppm for carbon and 31.00 ppm for hydrogen).

Table 1. Selected Bond Lengths (Å) and Angles (deg) of the Redetermined Structure of $Mo(bd)_3$

	major (sof 0.77)		minor (sof 0.23)
Mo−C1	2.284(2)	Mo−C2′	2.330(5)
Mo−C2	2.325(2)	Mo−C1′	2.273(6)
C1−C2	1.414(4)	C1′−C2′	1.414(7)
C2−C2A	1.403(5)	C2′−C2′A	1.388(9)
C1−C2−C2A	119.20(15)	C1′−C2′−C2′A	119.7(4)

Crystal Data and Structure Determination for $Mo(bd)_3$. The data set was collected using an oil-coated shock-cooled crystal[29] on a Kappa-CCD diffractometer with Mo Kα ($\lambda = 71.073$ pm) radiation equipped with a low-temperature device at 173(2) K. The structure was solved by direct methods (SHELXS-NT 97)[30] and refined by full-matrix least-squares methods against F^2 (SHELXL-NT 97).[31] *R* values defined as $R1 = \sum||F_o| - |F_c||/\sum|F_o|$, $wR2 = [\sum w(F_o^2 - F_c^2)^2/\sum w(F_o^2)^2]^{0.5}$, $w = [\sigma^2(F_o^2) + (g_1P)^2 + g_2P]^{-1}$, $P = 1/3[\max(F_o^2,0) + 2F_c^2]$. **$Mo(bd)_3$**: $C_{12}H_{18}Mo$, $M = 258.20$, hexagonal, space group $P6_3/m$, $a = b = 7.2142(10)$ Å, $c = 11.802(2)$ Å, $V = 531.94(15)$ Å^3, $Z = 2$, $\rho_{calc} = 1.612$ Mg/m^3, $\mu = 1.184$ mm^{-1}, $F(000) = 264$; 3263 reflections measured, 451 unique, $R(int) = 0.0214$, wR2(all data) = 0.0444, $R1(I > 2\sigma(I)) = 0.0190$, $g_1 = 0.0204$, $g_2 = 0.2754$, 53 restraints and 40 parameters. Absorption correction MULTISCAN. The site occupation factors (sof's) of the disordered butadiene ligands were refined freely to 0.77 and 0.23, respectively. All non-hydrogen atoms were refined anisotropically. The hydrogen atoms were geometrically idealized and refined using a riding model. Selected bond lengths and angles of $Mo(bd)_3$ can be found in Table 1. Crystallographic data for the structure has been deposited with the Cambridge Crystallographic Data Centre as supplementary publication no. CCDC-188011. Copies of the data can be obtained free of charge on application to CCDC, 12 Union Road, Cambridge CB2 1EZ, UK [fax: (Internat.)+44-1223/336-033, e-mail: deposit@ccdc. cam.ac.uk].

Results and Discussion

Computed Structures. At all four computational levels employed, the experimental observation of a C_{3h} symmetrical structure with trigonal prismatic coordination of the metal by the terminal carbon atoms (C_1) of the three butadiene ligands has been confirmed (see Figure 2, which also shows the atom labeling used). The three electron-correlated computational levels (MP2,

(16) Dolg, M.; Wedig, U.; Stoll, H.; Preuss, H. *J. Chem. Phys.* **1987**, *86*, 866. Andrae, D.; Häussermann, U.; Dolg, M.; Stoll, H.; Preuss, H. *Theor. Chim. Acta* **1990**, *77*, 123.
(17) Bergner, A.; Dolg, M.; Küchle, W.; Stoll, H.; Preuss, H. *Mol. Phys.* **1993**, *80*, 1431.
(18) d-Type polarization functions have been taken from: *Gaussian Basis Sets for Molecular Calculations*; Huzinaga, S., Ed.; Elsevier: New York, 1984.
(19) Godbout, N.; Salahub, D. R.; Andzelm, J.; Wimmer, E. *Can. J. Chem.* **1992**, *70*, 560.
(20) (a) Reed, A. E.; Weinhold, F. *J. Chem. Phys.* **1985**, *83*, 1736. (b) Reed, A. E.; Curtiss, L. A.; Weinhold, F. *Chem. Rev.* **1988**, *88*, 899.
(21) Glendening, E. D.; Weinhold, F. *J. Comput. Chem.* **1998**, *19*, 593.
(22) Glendening, E. D.; Badenhoop, J. K.; Reed, A. E.; Carpenter, J. E.; Weinhold, F. *NBO-4.M program*; Theoretical Chemistry Institute, University of Wisconsin, 1998.
(23) Malkin, V. G.; Malkina, O. L.; Casida, M. E.; Salahub, D. R. *J. Am. Chem. Soc.* **1994**, *116*, 5898.
(24) deMon program: (a) Salahub, D. R.; Fournier, R.; Mlynarski, P.; Papai, I.; St-Amant, A.; Ushio, J. In *Density Functional Methods in Chemistry*; Labanowski, J., Andzelm, J., Eds.; Springer: New York, 1991. (b) St-Amant, A.; Salahub, D. R. *Chem. Phys. Lett.* **1990**, *169*, 387.
(25) Malkin, V. G.; Malkina, O. L.; Eriksson, L. A.; Salahub, D. R. In *Modern Density Functional Theory: A Tool for Chemistry; Theoretical and Computational Chemistry*; Seminario, J. M., Politzer, P., Eds.; Elsevier: Amsterdam, 1995; Vol. 2.
(26) (a) Perdew, J. P.; Wang, Y. *Phys. Rev. B* **1992**, *45*, 13244. (b) Perdew, J. P. *Electronic Structure of Solids*; Ziesche, P., Eischrig, H., Eds.; Akademie Verlag: Berlin, 1991. (c) Perdew, J. P.; Chevary, J. A.; Vosko, S. H.; Jackson, K. A.; Pederson, M. R.; Singh, D. J.; Fiolhais, C. *Phys. Rev. B* **1992**, *46*, 6671.
(27) Kutzelnigg, W.; Fleischer, U.; Schindler, M. *NMR−Basic Principles and Progress;* Springer: Heidelberg, 1990; Vol. 23, p 165ff.
(28) Edmiston, C.; Ruedenberg, K. *Rev. Mod. Phys.* **1963**, *35*, 457−465; *J. Chem. Phys.* **1965**, *43*, 597−602. Boys, S. F. *Quantum Theory of Atoms, Molecules and the Solid State*; Löwdin, P. O., Ed.; Academic Press: New York, 1966; p 253ff. This procedure is often erroneously attributed to: Foster, J. M.; Boys, S. F. *Rev. Mod. Phys.* **1963**, *35*, 457−465.
(29) Kottke, T.; Stalke, D. *J. Appl. Crystallogr.* **1993**, *26*, 615. Kottke, T.; Lagow, R. J.; Stalke, D. *J. Appl. Crystallogr.* **1996**, *29*, 465. Stalke, D. *Chem. Soc. Rev.* **1997**, *27*, 171.
(30) Sheldrick, G. M. *Acta Crystallogr. Sect. A* **1990**, *46*, 467.
(31) Sheldrick, G. M. *SHELXL-NT 97, Program for Crystal Structure Refinement*; Göttingen, 1997.

Table 2. Computed Structural Parameters of $Mo(bd)_3$ Compared to Old and New Experimental Data[a]

	HF	MP2	BP86	B3LYP	expt, old[c]	expt, new[d]
Mo−C1	2.314	2.262	2.294	2.302	2.29(1) [2.301(8)]	2.284(2), 2.273(6)
Mo−C2	2.349	2.354	2.360	2.367	2.29(1) [2.317(7)]	2.325 (2), 2.330 (5)
C1−C2	1.408	1.441	1.434	1.427	1.32(2) [1.336(11)]	1.414(4), 1.414(7)
C2−C2A	1.395	1.398	1.408	1.401	1.55(3) [1.560(18)]	1.403(5), 1.388(9)
C1−H1	1.076	1.087	1.094	1.087	1.14(8) [1.00[e]]	
C1−H2	1.077	1.091	1.098	1.089	0.96(10) [1.00[e]]	
C2−H3	1.074	1.087	1.094	1.086	1.12(10) [1.00[e]]	
C1−C2−C2A	120.3	119.0	119.4	119.7	114.84(88)	119.20(15), 119.7(4)
H1−C1−C2	118.4	117.1	117.7	118.0	121.99(5.30)	
H2−C1−C2	117.3	116.9	117.3	117.2	119.10(6.33)	
H3−C2−C2A	118.3	119.0	118.7	118.5	125.24(5.32)	
$\sum\alpha$(C1)[b]	349.7	348.3	348.3	348.8	349.9	

[a] Distances in Å, angles in deg. Cf. Figure 2 for atom labeling. [b] Sum of angles around C1. [c] Results from ref 5, with more recent data from ref 2 in brackets. [d] This work, two inequivalent positions of disordered model. [e] C−H distances were kept fixed at this value.

Table 3. Structural Comparison between Free Ligands and Complexes[a]

	bd[b]	$Mo(bd)_3$	$W(bd)_3$[c,d]	C_4F_6[b]	$Mo(C_4F_6)_3$	dmbd[b,e]	$Mo(dmbd)_3$[f]
Mo−C1		2.294	2.285(2.336)		2.256		2.262
Mo−C2		2.360	2.381(2.395)		2.458		2.427
C1−C2	1.351	1.434	1.444(1.434)	1.352	1.466	1.354	1.447
C2−C2A	1.470	1.408	1.404(1.410)	1.461	1.392	1.498	1.415
C1−X1	1.093	1.094	1.095(1.094)	1.320	1.346	1.094	1.096
C1−X2	1.095	1.098	1.099(1.098)	1.320	1.361	1.094	1.098
C2−X3	1.097	1.094	1.095(1.094)	1.349	1.327	1.515	1.510
C1−C2−C2A	127.3	119.4	118.9(120.0)	130.8	120.9	123.3	117.3
X1−C1−C2	121.0	117.7	116.5(117.4)	122.5	112.3	120.8	116.0
X2−C1−C2	122.4	117.3	117.3(118.0)	125.2	116.0	122.8	117.1
X3−C2−C2A	115.0	118.7	118.9(118.5)	113.0	118.6	117.6	122.1
$\sum\alpha$(C1)[g]	360.	348.3	347.0(349.1)	360.	336.4	360.	345.7

[a] BP86 computational results. Distances in Å, angles in deg. Cf. Figure 2 for atom labeling. [b] The *cis* conformer has been enforced. [c] Experimental data for tris(2,3-dimethylbutadiene)tungsten: W−C1 = 2.24(1) Å, W−C2 = 2.42(1) Å, C1−C2 = 1.48(1) Å, C2−C2A = 1.38(1) Å (cf. ref 6). [d] Quasirelativistic ECP results with nonrelativistic ECP results in parentheses. [e] 2,3-Dimethylbutadiene. [f] Tris(2,3-dimethylbutadiene)molybdenum; experimental data: Mo−C1 = 2.252(3) Å, Mo−C2 = 2.402(2) Å, C1−C2 = 1.440(3) Å, C2−C2A = 1.400(3) Å (cf. ref 6). [g] Sum of H−C1−H and H−C1−C angles.

BP86, B3LYP) give very similar results for bond lengths and angles (Table 2; MP2 gives slightly shorter Mo−C bonds and slightly larger variations between terminal and central positions than the DFT methods). The HF results are similar qualitatively but deviate somewhat quantitatively from the other three levels. We will thus in the following concentrate on the correlated methods, with the most economical gradient-corrected DFT level (BP86) being the method of choice for our calculations on the larger, substituted complexes. Additional calculations on $W(bd)_3$ indicate similar agreement between different computational methods (cf. Supporting Information).

While the calculations confirm the prismatic coordination arrangement, they disagree significantly with the previously reported, crystallographically determined dimensions[2,5] (cf. Table 2). In particular, the terminal C1−C2 and central C2−C2A bond lengths are very similar, with the central bond generally being ca. 0.03−0.04 Å shorter. The terminal Mo−C1 distances are calculated to be ca. 0.07−0.09 Å shorter than the central Mo−C2 distances. These results contradict the "butadiene-like" C−C distances and equal Mo−C distances reported.[2,5] However, they agree much better with the structures found[6] for tris(2,3-dimethylbutadiene)molybdenum and -tungsten (cf. Table 3; the methyl substituents apparently give rise to slightly enhanced back-bonding).

Our previous experience with related systems, e.g., with a series of d^0−d^2 hexamethyl complexes,[9,10] shows that the level of agreement we find here between MP2 and different DFT calculations will persist at even higher (e.g., coupled cluster) theoretical levels. The discrepancies relative to the previous experimental data are clearly outside the expected error margins of the quantum chemical calculations. Closer inspection reveals also that the "experimental" C−H distances[2] are unreasonable (Table 2). This points clearly to problems with the crystallographic data, which had been obtained at room temperature and exhibited suspiciously large temperature factors.[5] We have therefore carried out a low-temperature single-crystal X-ray diffraction study on $Mo(bd)_3$. The results are reported further below. Other structural details revealed by the quantum chemical calculations are the significant pyramidalization at the C1 carbon atoms and the smaller C1−C2−C2A angles (Table 2), compared to the planar free ligand (Table 2). This points to rehybridization at the C1 atoms, due to partial Mo−C1 σ-bonding (cf. bonding considerations below).

Table 3 compares the most important BP86-optimized structural parameters of $M(bd)_3$ (M = Cr, Mo, W), $Mo(dmbd)_3$ (dmbd = 2,3-dimethylbutadiene), the perfluorinated analogue $Mo(C_4F_6)_3$, and the corresponding free ligands. The structures of $Mo(bd)_3$ and $W(bd)_3$ are similar. The tungsten complex exhibits an even slightly larger difference between M−C1 and M−C2 distances (ca. 0.10 Å instead of ca. 0.07 Å), and the difference between the C1−C2 and C2−C2A distances is also very slightly larger. These structural details suggest that back-bonding is even more pronounced for the 5d tungsten homologue. The nonrelativistic ECP calculations on $W(bd)_3$ give a structure suggesting less back-bonding. Obviously, the enhanced back-bonding for

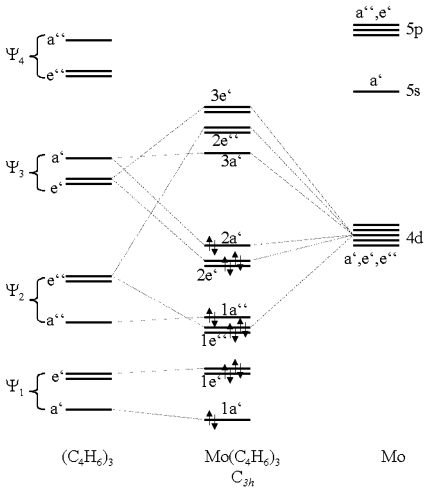

Figure 3. MO diagram for $Mo(bd)_3$, based on Kohn−Sham MOs (BP86 level).

$W(bd)_3$ relative to $Mo(bd)_3$ is due to the relativistic expansion[32] of 5d relative to 4d orbitals. For both $Mo(bd)_3$ and $W(bd)_3$, comparison with free butadiene (in its *cis* conformation) shows the very large equalization, and even partial inversion, of the C−C bond lengths, as found previously for the dimethylbutadiene complexes.[6] Indeed, our calculations for $Mo(dmbd)_3$ (Table 3) are in close agreement with the experimental results, thus showing the adequacy of the computational methods employed. In the substituted complex, the differentiation between the Mo−C1 and Mo−C2 distances is even somewhat more pronounced than for the parent compound. Both C1−C2 and C2−C2A distances are slightly expanded, and thus the calculations confirm the somewhat shorter C2−C2A than C1−C2 bond length.

We have included the perfluorinated system $Mo(C_4F_6)_3$ in our study (Table 3), as we expected that the electronegative fluorine substituents should further enhance back-bonding into ligand π^* orbitals. Indeed, the Mo−C1 distances are calculated to be ca. 0.04 Å shorter than in the parent $Mo(bd)_3$. Most notably, the central Mo−C2 distances have expanded by almost 0.10 Å. Starting from the bonding viewpoint of fused metallacyclopentenes (see below), this suggests that the electronegative fluorine substituents diminish donation from the C2−C2A π-bond to the metal. From the alternative "π-bonded diolefin" viewpoint, the π-back-bonding into the π^* MOs of perfluorobutadiene appears to be enhanced significantly (cf. below). Consequently, the C1−C2 bond is slightly longer than in $Mo(bd)_3$. The C2−C2A bond is slightly shorter, but this is to some extent already true for the free ligand. Pyramidalization at C1 is also still more pronounced than in $Mo(bd)_3$.

We have also attempted to optimize the structure of $Cr(bd)_3$ at the same computational levels as for the other complexes. However, when we relaxed the symmetry restrictions to C_s symmetry during the optimization, we observed dissociation of one or two ligands as cyclobutene. These results make the existence of $Cr(bd)_3$ appear unlikely. The instability is probably due to insufficient back-bonding from the metal 3d orbitals, as well as to steric crowding around the small chromium center.

(32) See, for example: Pyykkö, P. *Chem. Rev.* **1988**, *88*, 563.

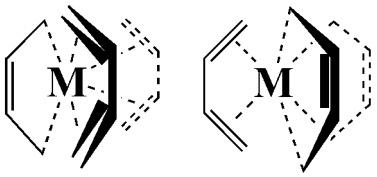

3, Mo^{II}, d^4 **4**, Mo^{IV}, d^2

Figure 4. Intermediate resonance structures for $Mo(bd)_3$.

Bonding Discussion. Figure 3 shows the MO diagram of $Mo(bd)_3$, based on the Kohn−Sham orbitals obtained at the BP86 level. The order of the frontier orbitals differs from those obtained in the extended-Hückel study of ref 5. The 2a′ MO has moved above the 2e′ set and becomes the HOMO. Correspondingly, the 3a′ MO is now below 2e″ and becomes the LUMO. These differences are not due to the different computational methods (DFT vs EHT) but due to the different structures employed (DFT-optimized in this work, "old" experimental data in ref 5). Using the older "experimental" structure, we arrive at the same ordering as Green et al.[5] Obviously, the equalization of C−C distances and the shorter Mo−C1 bond allow a further strengthening of the interactions of e′ relative to a′ MOs.

In an attempt to evaluate the importance of resonance structures **1** and **2** in Figure 1, we have carried out separate NBO analyses, in which we have forced strictly localized NBO Lewis structures corresponding to **1** and **2**, respectively (cf. Figure 1). Neither of these two resonance structures describes the one-particle density matrix particularly well. While **1** alone is able to describe ca. 95.5% of the one-particle density, **2** can account for ca. 97.0%. Experience shows that in well-localized cases, the optimal Lewis structure usually accounts for >99.5%.[20] The present numbers clearly indicate a delocalized electronic situation, which is somewhat better approximated by the Mo^{VI} case **2** than by the Mo^0 case **1**. One may also envision the intermediate resonance structures **3** and **4** shown in Figure 4, in which either one or two of the ligands are viewed as dianionic 2,3-butene-1,2-diyls, leading to formal oxidation states Mo^{II} and Mo^{IV}, respectively. When **3** is enforced, it decribes 96.2% of the one-particle density, whereas **4** is able to account for 96.9%. While this is intermediate between the performance of the initial, extreme resonance structures **1** and **2**, we have to keep in mind that permutation leads to three equivalent forms **3** and three equivalent forms **4**. This suggests that these intermediate resonance structures may have a particularly large weight in the overall wave function. To evaluate this in more detail, we have carried out an NRT analysis,[21] which expresses the one-particle density matrix by a superposition of different NBO resonance structures. This has been shown to provide a very interesting link between the NBO expansion and ideas based on valence bond theory.[33] Among other things, NRT analyses have been used in the context of hypervalency in main group chemistry. Our current experience of NRT with transition metal complexes indicates frequently difficult convergence and a large sensitivity to the initial NBO Lewis structures provided. After

(33) Suidan, L.; Badenhoop, J. K.; Glendening, E. D.; Weinhold, F. *J. Chem. Educ.* **1995**, *72*, 583.

Table 4. Calculated NPA Charges[a]

	bd[b]	$Mo(bd)_3$	$W(bd)_3$	dmbd[b,c]	$Mo(dmbd)_3$[d]	C_4F_6[b]	$Mo(C_4F_6)_3$
M		0.070	0.375(0.180)		0.156		−0.218
C1	−0.403	−0.556	−0.608(−0.567)	−0.406	−0.561	0.708	0.615
C2	−0.267	−0.213	−0.220(−0.222)	−0.055	−0.003	0.171	0.316
X1	0.224	0.256	0.259(0.256)	0.219	0.249	−0.289	−0.310
X2	0.211	0.243	0.246(0.243)	0.214	0.241	−0.292	−0.321
X3	0.234	0.259	0.260(0.260)	0.028[e]	0.047[e]	−0.297	−0.264

[a] BP86//BP86. Cf. Figure 2 for atom labeling. [b] The *cis* conformer has been forced. [c] 2,3-Dimethylbutadiene. [d] Tris(2,3-dimethylbutadiene)molybdenum. [e] Charge of CH_3 group.

many tests, we found that in a multireference treatment based on all four alternatives shown in Figures 1 and 4, the extreme resonance structures **1** and **2** obtain negligible weights. A multireference treatment based on the set of six resonance structures described by **3** and **4** (Figure 4) generally indicates a particularly large weight of **4** (ca. 10% for each of the three permutations, adding up to ca. 30%), augmented by many other, considerably smaller contributions from alternative resonance structures (including resonance structures with unsymmetrically bonded ligands and with lone pairs on C1). These analyses show clearly that bonding is highly delocalized (as one might expect from the MO diagram in Figure 3). Due to significant back-bonding, resonance structures with one or more metallacyclopentene rings obtain significant weight. The overall situation appears to be most closely approximated by the sum of intermediate resonance structures **4**, which correspond to a formal Mo^{IV} oxidation state and a d^2 configuration. Notably, not only a d^0 configuration but also a formal low-spin d^2 configuration is consistent with a trigonal prismatic arrangement[9] (for example, calculations predict a regular trigonal prismatic structure for the d^2 complex $Os(CH_3)_6$[10d]). In agreement with this bonding picture, the natural bond orders arising from the final "multireference" NRT analyses are Mo−C1 0.63, Mo−C2 0.05, C1−C2 1.55, C2−C2′ 1.32.

Table 4 summarizes charges obtained from natural population analyses (NPA) for several of the ligands and complexes studied. Metal charges are relatively small for all complexes, thus supporting the rather delocalized bonding situation discussed above. The large covalency does, however, not contradict the much higher formal oxidation states required by resonance structures such as **4**. For example, NPA metal charges for the formal M^{VI} complexes $M(CH_3)_6$ have been calculated at the same computational level to be 0.793 and 1.148 for Mo and W, respectively.[34] The generally somewhat larger positive charge for the tungsten complexes may be traced partly to the relativistic expansion of the tungsten 5d orbitals[34] (cf. nonrelativistic results in parentheses). The negative metal charge for $Mo(C_4F_6)_3$ indicates particularly pronounced back-bonding. Comparing the charges within the free and coordinated ligands, the polarization of charge toward the terminal carbon atoms (C1) is most notable. This is consistent with the partial rehybridization of these atoms toward sp^3 and with the partial formation of a metal−alkyl M−C bond. In contrast, charge is withdrawn from the central carbon atoms (C2). Furthermore, the charges at the substituent atoms are also modified, but the outcome is rather different for, for example, hydrogen or fluorine substituents. Generally, the population analyses indicate significant charge transfer within the ligands upon coordination, consistent with pronounced donor and acceptor bonding.

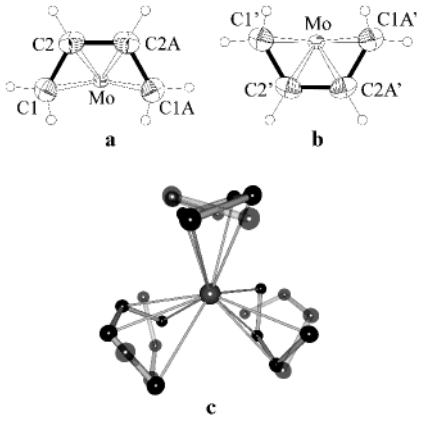

Figure 5. Redetermined crystal structure of $Mo(bd)_3$. (a) Butadiene ligand with the major site occupation factor. (b) Butadiene ligand with the minor occupancy. Anisotropic displacement parameters are at the 50% probability level. (c) Disorder of the ligands around the molybdenum atom (0.77 sof solid, 0.23 sof transparent).

Crystal Structure of $Mo(bd)_3$. Bond distances and angles are summarized in Table 1. The structure was refined in the previously published hexagonal space group $P6_3/m$ with the Mo atom at the 3-fold axis placed on the mirror plane. This gives rise to half a butadiene ligand in the asymmetric unit completed by the mirror plane orthogonal to the central C−C bond. The three η^4-bonded ligands are orientated clockwise along the 3-fold axis. During refinement of the structure from low-temperature data it was immediately obvious that a second orientation of the ligands with a lower sof is present. In this arrangement the ligands are arranged in an anticlockwise direction along the 3-fold axis (sof 0.23); see Figure 5. Both domains were refined by geometrical similarity restraints. Refinement of the structure in the lower symmetric space group $P6_3$ leads to the same disorder and gave the same results. We suspect that in the published structure this disorder was not modeled successfully and gave an overall "smeared" image of the ligands, resulting in wrong bond distances with high esd's. In the redetermined low-temperature structure the adp's show basically isotropic behavior and the esd's are reduced by the factor of 10 compared with the published structure. A related type of disorder as identified here for $Mo(bd)_3$ has been found previously for the complex $CpNb(bd)_2$.[35]

(34) Kaupp, M. *Chem. Eur. J.* **1998**, *4*, 1678.

(35) Herberich, G. E.; Englert, U.; Linn, K.; Roos, P.; Runsink, J. *Chem. Ber.* **1991**, *124*, 975.

Table 5. Computed Ligand NMR Chemical Shifts[a] (in ppm vs TMS); Comparison with Experimental Data

	bd[b] calc str BP86	$Mo(bd)_3$ calc str BP86	$Mo(bd)_3$ exptl str[c] old (new)	$W(bd)_3$ calc str BP86	dmbd[b,d] calc str BP86	$Mo(dmbd)_3$[e] calc str BP86
C1 calc	113.5	49.6	29.1	44.3	112.9	54.9
	(119.5)		(49.1)		(112.4)	
exptl	117.5	41.4	41.4	33.7	113.05	49.5
C2 calc	133.0	105.8	98.8	107.3	150.7	114.8
	(139.2)		(100.9)		(145.8)	
exptl	137.8	102.2	102.2	103.4	143.60	112.1
X1 calc	5.42	1.48	−2.42	1.22	4.89	1.10
	(5.18)		(1.55)		(5.05)	
exptl	5.08	1.50	1.50	1.35	5.055	1.32
X2 calc	5.48	0.31	1.33	0.21	4.92	−0.44
	(5.39)		(0.14)		(5.24)	
exptl	5.18	0.37	0.37	0.26	4.968	−0.41
X3 calc	5.86	4.84	4.72	4.94	22.8[f]	22.6[f]
	(6.13)		(4.71)		(21.6)	
exptl	6.31	4.52	4.52	4.61	20.65[g]	20.3[g]

[a] SOS-DFPT/PW91 results at optimized structures from Table 3. ^{13}C and ^{1}H shifts relative to TMS. Experimental data from refs 6, 38, as well as from: Jolly, P. W.; Mynott, R. *Adv. Organomet. Chem*. **1982**, *19*, 257. Hesse, M.; Meier, H.; Zeeh, B. *Spektroskopische Methoden in der Organischen Chemie*, 5th ed.; Georg Thieme Verlag: Stuttgart, 1995. [b] Calculated free-ligand values for *cis* conformer, with *trans*-conformer results in parentheses. [c] Calculation at the "old" experimental structure of ref 5. Provided in parentheses are results with the "new" structure parameters of the disordered model (major occupancy, sof 0.77), augmented by BP86-optimized hydrogen positions. [d] 2,3-Dimethylbutadiene. [e] Tris(2,3-dimethylbutadiene)molybdenum. [f] ^{13}C shift. Average calculated methyl ^{1}H shifts are 1.64 and 1.61 ppm for dmbd and $Mo(dmbd)_3$, respectively. [g] ^{13}C shift. Experimental methyl ^{1}H shifts are 1.92 and 1.64 ppm for dmbd and $Mo(dmbd)_3$, respectively.[6]

Calculated NMR Chemical Shifts. Coordination shifts, i.e., changes in NMR chemical shifts between free and coordinated ligands, also provide valuable information on the bonding situation. Moreover, comparison of computed and measured shifts allows a further check of the correctness of the calculated structures.[36] The combination of density functional theory with quasi-relativistic ECPs on the heavy metal has been shown previously to allow the accurate calculation of ligand NMR chemical shifts in transition metal complexes.[37] Table 5 summarizes ^{13}C and ^{1}H chemical shifts, calculated within the SOS-DFPT/IGLO approach. The agreement between calculations and experiment is of similar quality for $Mo(bd)_3$, $W(bd)_3$, and $Mo(dmbd)_3$. Deviations are within the expected accuracy for the SOS-DFPT approach, density functional, and basis sets employed. In particular, the calculations reproduce the significant coordination shifts to low frequencies (high fields) for the terminal carbon atoms (C1), as well as for their attached hydrogen atoms (H1, H2). The low-frequency coordination shifts for the central carbon atoms (C2) are also reproduced by the calculations. Low-frequency coordination shifts are generally observed for olefin ligands, but their substantial magnitude in the present cases confirms the significant amount of back-bonding, which in turn is consistent with large structural modifications of the ligands. The shifts for $Mo(bd)_3$ computed with the old, inaccurate structural data are in considerably inferior agreement with experiment than the results obtained with quantum chemically optimized structures (Table 5). This holds in particular for the atoms H1 and H2 and provides a further confirmation of the incorrectness of the older structure data. We have also used the main structure parameters of the major occupancy (sof 0.77) of the present disordered model, augmented by quantum chemically calculated hydrogen positions (BP86 results). In this case, significantly improved chemical shifts for all nuclei are obtained, comparable to the results with fully quantum chemically optimized structures (Table 5).

In a detailed ^{1}H NMR study, Benn and Schroth used both coupling constants and coordination chemical shifts to discuss the bonding in early transition metal butadiene complexes, including $M(bd)_3$ (M = Mo, W).[38] They concluded that bonding in both complexes exhibits significant contributions from metallacyclopentene resonance structures, consistent with our computed structures and chemical shifts, and with the bonding discussion above.

Conclusions

Detailed quantum chemical calculations at different computational levels have confirmed the trigonal prismatic metal coordination in tris(butadiene)molybdenum and related complexes. However, the calculations show clearly a pronounced equilibration of C−C distances within the ligands, as well as significantly shorter terminal than central M−C bonds. Comparison of calculated and experimental NMR chemical shifts provides additional support for the correctness of the computed structures.

While these results are consistent with the expectation of significant back-bonding, they are in sharp disagreement with the conclusions from previous X-ray structure determinations for $Mo(bd)_3$, which have given C−C bond lengths essentially as for the free butadiene ligand and almost equal Mo−C distances. We have therefore carried out a low-temperature X-ray diffraction study on $Mo(bd)_3$ and modeled a disorder, which has previously not been identified. Refinement of this disorder permits deconvoluting the "smearing" of superimposed ligands and gives much more reliable distances now in tune with the quantum chemical results.

Having thus confirmed the validity of the quantum chemical structure determinations, we have analyzed

(36) Bühl, M. In *Encyclopedia of Computational Chemistry*; Schleyer, P. v. R., Ed.; Wiley-Interscience: New York, 1998.

(37) For reviews see, for example: Kaupp, M.; Malkina, O. L.; Malkin, V. G. In *Encyclopedia of Computational Chemistry*; Schleyer, P. v. R., Ed.; Wiley-Interscience: New York, 1998. Bühl, M.; Kaupp, M.; Malkin, V. G.; Malkina, O. L. *J. Comput. Chem*. **1999**, *20*, 91.

(38) Benn, R.; Schroth, G. *J. Organomet. Chem*. **1981**, *228*, 71.

the bonding situation by various methods. NBO and NRT analyses confirm significantly delocalized bonding in all of the butadiene complexes studied. NRT favors resonance structures with more metallacyclopentene than "π-bonded diolefin" character, in agreement with the optimized structures. Similar analyses might be useful for other transition metal complexes with delocalized bonding situations. A computed MO diagram for $Mo(bd)_3$ differs somewhat from earlier studies that were based on incorrect structural data.

Acknowledgment. M.K. is grateful to Dr. Frank Weinhold (University of Wisconsin) for providing his NBO4.M code. This work was supported by Deutsche Forschungsgemeinschaft, the Graduiertenkolleg "Elektronendichte: Theorie und Experiment" at Universität Würzburg, the Fonds der Chemischen Industrie, and EPSRC.

Supporting Information Available: Table S1 provides a comparison of optimized internal coordinates for $W(bd)_3$ at different computational levels. This material is available free of charge via the Internet at http://pubs.acs.org.

OM020525V